DE GRUYTER Pure Appl. Chem. 2019; 91(2): 271–288

Special topic

Katharina Kohse-Höinghaus*

A new era for combustion research[a]

https://doi.org/10.1515/pac-2018-0608

Abstract: Current topics in combustion chemistry include aspects of a changing fuel spectrum with a focus on reducing emissions and increasing efficiency. This article is intended to provide an overview of selected recent work in combustion chemistry, especially addressing reaction pathways from fuel decomposition to emissions. The role of the molecular fuel structure will be emphasized for the formation of certain regulated and unregulated species from individual fuels and their mixtures, exemplarily including fuel compounds such as alkanes, alkenes, ethers, alcohols, ketones, esters, and furan derivatives. Depending on the combustion conditions, different temperature regimes are important and can lead to different reaction classes. Laboratory reactors and flames are prime sources and targets from which such detailed chemical information can be obtained and verified with a number of advanced diagnostic techniques, often supported by theoretical work and simulation with combustion models developed to transfer relevant details of chemical mechanisms into practical applications. Regarding the need for cleaner combustion processes, some related background and perspectives will be provided regarding the context for future chemistry research in combustion energy science.

Keywords: biofuels; combustion; combustion models; Distinguished Women in Chemistry and Chemical Engineering; energy; fuels; pollutant formation; reaction mechanisms.

Introduction

Please allow me to start with an anecdote. Some 10 years ago, on a flight from Frankfurt to San Francisco, my seat neighbor talked to me about his job in solar energy research and development. When asked about my own profession, I revealed to work in combustion science, he claimed: “Well, that science will probably die out with you!” – to which I could only answer that my peers might still be around until his results could make our plane fly 300+ passengers transatlantic with solar energy. Ten years later, the scales between solar and combustion energy have not changed regarding mass air transportation, and they are not likely to do so within decades to come, because of the well-known energy density or range advantage of liquid energy carriers. Of course, this comparison is unrealistic, with solar energy better suited for stationary power generation than for direct aircraft propulsion. However, solar energy and hydrocarbon fuel combustion may be combined by using (surplus) sustainable electric power such as from solar and wind energy to synthesize liquid chemicals such as transportation fuels in power-to-liquid approaches [1–3] that may serve to integrate energy storage and chemical production.

Internal combustion (IC) engines for road transportation may appear challenged after several countries have announced to ban their production or sales in the future, partly as a reaction to emission scandals, and partly because solutions such as electric propulsion are more easily adopted for ground than for air transport. Nevertheless, as shown in Fig. 1, range density (in km/L) and specific range (in km/kg) of conventional liquid fuels such as diesel and gasoline are still hard to match [4], neither by biofuels such as ethanol or isobutanol,

---

[a] **Note in proof:** Since submission of this article, Johansson and coauthors (K. O. Johansson, M. P. Head-Gordon, P. E. Schrader, K. R. Wilson, H. A. Michelson, Science 361, 997, 2018) have reported a new mechanism that may resolve some of the pertinent questions regarding soot formation.

***Corresponding author: Katharina Kohse-Höinghaus,** Department of Chemistry, Bielefeld University, Universitätsstraße 25, Bielefeld D-33615, Germany, Phone: +49 5211062052, E-mail: kkh@uni-bielefeld.de

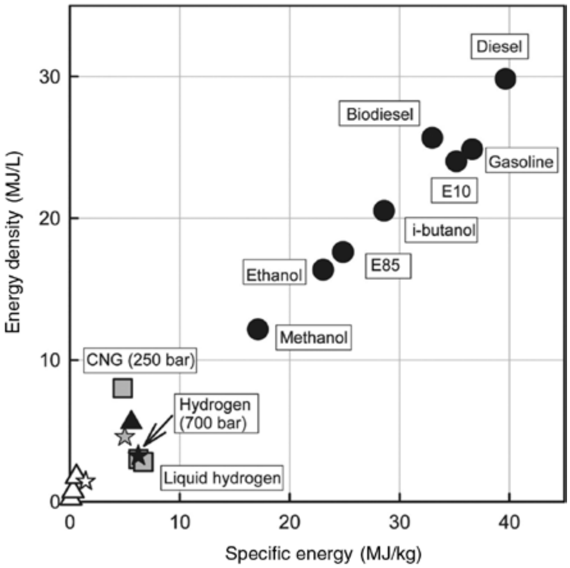

Fig. 1: Energy density (MJ/L) and specific energy (MJ/kg) for selected fuels (includes both fuel and fuel storage system). Circles (squares) are fuels that are liquid (gaseous) under ambient conditions. Batteries are shown as triangles, with open triangles representing current battery chemistries (Li-ion, nickel–metal hydride, lead–acid) and the filled triangle representing the projected performance of a Li–oxygen battery. Solid hydrogen storage systems are shown as stars (open: complex metal hydrides, black: adsorbents, gray: chemical hydrides). CNG is compressed natural gas and E10 and E85 is gasoline with 10 and 85 % ethanol. Reprinted from Fig. 2 (left panel) in Ref. [4], available at https://pubs.acs.org/doi/abs/10.1021/ed3004269, with permission by the American Chemical Society to where inquiries for further permission regarding this material should be directed.

nor by fuels that are gaseous at ambient conditions including natural gas and hydrogen, nor by current battery technology.

Against the background of a changing energy portfolio and a potential “mobility revolution” with probable shifts towards more electrification, shared mobility concepts, and autonomous driving [5], it is instructive to consider extrapolations to the future from the current status for transportation as, for example, given in Ref. [5]. Transport (air, sea, and ground) currently consumes about 20 % of global primary energy. An “evolving transition” scenario [5] without disruptive changes assumes more than duplicated transportation demand until 2040 as a result of growing prosperity in emerging economies, with a less steep increase in energy consumption for this purpose by “only” 25 % due to increased efficiency. Fuel demand in the transport sector is expected to remain dominated by oil, but from 94 % today, the oil-based fuel share may decrease to about 85 % by 2040, with the remaining 15 % including natural gas, electricity, and other fuels such as biofuels and hydrogen [5]. Passenger car numbers might nearly double to about 2 billion by 2040, with an assumed share of 300 million electric cars including battery-electric vehicles and plug-in hybrids [5], and the remaining more than a billion assumed as powered by internal combustion engines. Indeed, consumer demand for cars has been increasing in countries with large populations such as China and India, as seen in Table 1 that reports the number of vehicles per 1000 people in selected areas of the world over the decade of

Table 1: Vehicles per thousand people for selected areas, adapted from Table 3.5 in Ref. [6].

Area (Year)	2005	2015
China	23.5	115.8
India	11.1	33.4
Europe, West	577.8	597.6
USA	837.2	820.1

For methodology and data sources, see the original publication.

2005–2015 [6]. Absolute numbers in China and India may seem low in comparison with the near-saturated situation in Western Europe and the USA. However, should more than a billion consumers in Asia adopt similar habits to those established in more industrialized regions, especially when using existing technology, the impact on carbon dioxide emission and regional air quality would be enormous.

Main challenges associated with combustion systems are their current dependence on fossil energy sources and their emissions, including carbon dioxide (CO_2) and commonly regulated pollutants such as carbon monoxide (CO), nitrogen oxides (NO_x), unburnt hydrocarbon species (HC), and particulate matter (PM) or soot. Numerous studies have addressed their importance related to current and future energy scenarios and their effects on climate, environment, air quality, and human health [7–9]. Although carbon dioxide has been the main focus of climate change concerns with respect to combustion processes, the highly important role of soot emissions has been recognized [10]. Understanding and monitoring sources and effects of particulate emissions is especially valuable in severely affected regions, as, for example, in China [11]. Energy efficiency is of key importance to reduce CO_2 emissions, and cleaner engine strategies such as low-temperature combustion (LTC) approaches are being developed [12] to alleviate the burden from NO_x and particulate emissions.

Combustion science faces exciting times in view of the global situation and changing boundary conditions. New regulations or even disruptive political decisions are unlikely to lead, on a global scale, to a rapid end of the combustion engine, especially in view of the huge numbers of existing systems and current infrastructure. Increasing diversity of the fuel mix is already foreseeable for the future, with a variety of energy conversion concepts including combustion systems and fuel cells using different gaseous and liquid energy carriers [13–15]. Such different energy carriers may also influence the way to provide electricity for batteries, for which some pertinent challenges must be addressed regarding their energy density, lifetime, charging infrastructure, and recycling. Hybrid propulsion concepts may continue to include battery–combustion systems or might involve battery–fuel cell combinations that should be as suited for automated driving in non-linear (e.g. stop-and-go) situations as for long-distance range [16]. Combustion science and engineering will have to play an important but changing role as an integrative part of a future energy, mobility, and industrial production scenario using machines adapted to the necessary but different power, temperature, and pressure requirements, including combustion devices such as gas turbines, industry burners, and advanced engines.

Fuel-specific reactivity, combustion models, and validation

A diverse fuel spectrum from various sources and feedstocks in combination with new engine concepts to enhance performance while reducing emissions – this challenging research and application direction goes along with an increasing demand for combustion chemistry information. Multiple data are required and include characteristics of the ignition and extinction behavior in addition to numerous physico-chemical properties as, for example, enthalpies, heat capacities, density, and viscosity. Conventional fuels such as gasoline, diesel, and kerosene are composed of hundreds of hydrocarbon species. Their components as well as those of synthetic alternatives may feature 4–20 carbon atoms and different (e.g. linear or branched) molecular structures, depending on the specific oil distillate or e.g. Fischer-Tropsch synthesis product for the intended purpose [17, 18]. It is not sufficient to consider a global oxidation reaction of the form: *fuel + oxygen → carbon dioxide + water* to describe and predict the specific reaction sequences and the nature and amount of potential pollutants. Many aspects of the formation reactions of NO_x [19, 20], polycyclic aromatic hydrocarbons (PAHs) as typical soot precursors [21–24], and soot [21–23, 25–27] from conventional fuels that can be considered as established today, are based on decades of research, but even these reaction mechanisms still involve challenges.

Reliable mechanisms for the combustion reactions – the release of the chemical energy stored in the fuel – should be able to predict the combustion behavior of realistic fuels under practical conditions with sufficient accuracy for design, optimization, and control. Models that represent the combustion reactions of multi-component, conventional hydrocarbon fuels are becoming increasingly available [28–32]. They may rely on surrogate mixtures [30, 32–35] with a few compounds representative of important fuel characteristics to keep the computational effort manageable. For example, the detailed chemical mechanism for C_7–C_{20} 2-methylalkanes in Ref. [18] already features about 7000 species and 31 400 reactions. A recent hybrid ("HyChem") modeling strategy by Xu et al. [31] is illustrated in Fig. 2. Their approach to the high-temperature combustion of realistic fuels addresses pyrolysis and oxidative reactions separately. They deal with the pyrolysis chemistry that determines the early fuel decomposition reactions by several lumped steps (i.e. not resolved on an elementary reaction basis) that describe the formation of the most important pyrolysis intermediates. These are treated so that the behavior is in agreement with experimental data, assuming that most conventional hydrocarbon fuels will form a few similar, important pyrolysis intermediates such as hydrogen, methane, ethene, propene, butenes, benzene, and toluene that can be quite accurately measured in dedicated experiments [31]. Then, the oxidation reactions of the pyrolysis products including decisive reactive radicals are considered in detail, relying on the similar chemistry for different fuel components that are represented in typical mechanisms of so-called foundational fuels.

Designing high-performance fuels for advanced engines demands reliable information on their ignition properties that are sensitively influenced by the fuel's molecular structure [36]. The fuel-specific reactivity as a function of temperature, pressure, and stoichiometry is also a factor in adverse, efficiency-limiting effects such as engine knock [28]. The initial fuel-specific destruction reactions significantly affect the further reaction pathways and thus the composition of the reactive mixture with its hundreds of intermediate species that are formed during the reaction progress towards its final products. Consequentially, pollutant-forming reactions that depend sensitively on the species composition along the reaction pathway can be highly fuel-structure-dependent. The large variety of potential biofuels adds to the molecular diversity. Biomass-derived oxygenated fuels, used as additives or neat biofuels, can exhibit different reactivity and can lead to different pollutant composition, especially within the HC fraction. The nature and position of the respective oxygen-containing functional group in such fuel molecules as alcohols, esters, (cyclic) ethers, aldehydes, ketones, and hetero-aromatic compounds can contribute to the formation of a non-negligible amount of fuel-specific, in part harmful or toxic carbonyl species [37–39]. Mechanisms that can predict ignition behavior and potential exhaust components must be suitably optimized [34] so that they can be incorporated into more comprehensive engine models with the aim to describe the entire combustion process from the fuel delivery to the exhaust [40]. Special challenges originate from the interaction of the chemistry with the turbulent flow field [41] and other difficulties, including high pressures and multi-phase environments that demand intensified research [42]. Reliable models of predictive quality are thus useful as a link between the molecular fuel structure and the behavior of these fuel components in a real engine.

The difference in reactivity of important fuel classes discussed above can be seen in Fig. 3 that displays the computed ignition delay time as a function of experimental values of the research octane number (RON) [32].

Rather than using individual fuel models, the authors rely on a multi-fuel kinetic mechanism "with the eventual goal to include every chemical component that is present in a practical fuel that has a large enough fractional concentration to influence the overall performance of that fuel in a practical engine" [32]. Their

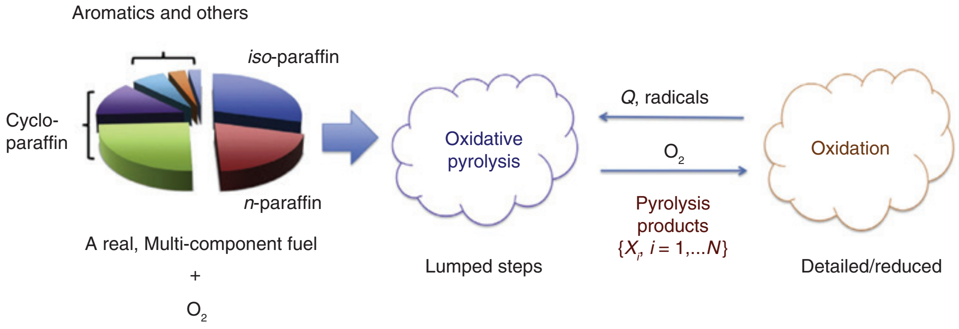

Fig. 2: "HyChem" modeling approach for a real multi-component fuel. Reprinted from Fig. 1 in Ref. [31] with permission by Elsevier/The Combustion Institute.

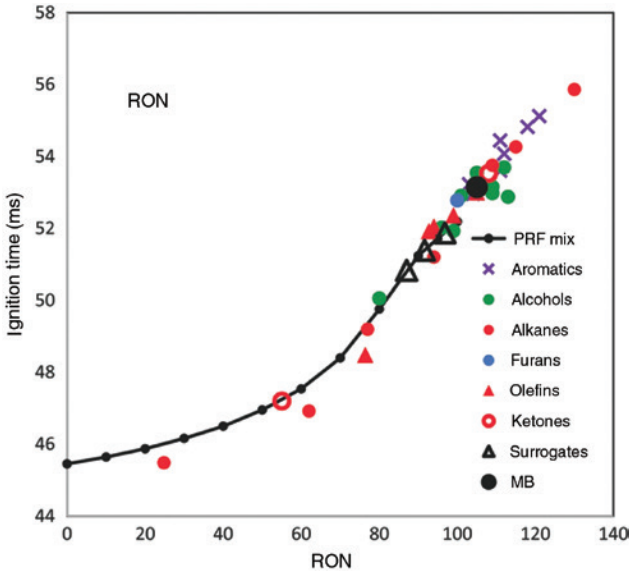

Fig. 3: Computed ignition delay time versus experimental values of the research octane number (RON) for different fuel classes [line: calibration curve for primary reference fuel (PRF), MB: methyl butanoate]; for details see the original paper. Reprinted from Fig. 4 in Ref. [32] with permission by the Royal Society of Chemistry.

computational approach is based upon two experimental engine cycles that were then modeled for each fuel along the entire pressure–time history, including both low- and high-temperature reactions. As seen in Fig. 3, the reactivity reflected in the fuels' ignition delay time varies in a consistent way with their octane numbers, and the computed values using the new approach agree well with the black calibration curve obtained for the primary reference fuel (PRF) components *n*-heptane and iso-octane [32]. The diagram includes numerous aromatics and thus extends the typical PRF range to high octane numbers. It is highly advantageous to use such a fundamental kinetic approach rather than engineering procedures based on single parameters such as octane numbers, as also discussed by Zhang et al. [43] in their recent study of the anti-knock tendency of substituted phenols as additives. They predicted the additives' behavior from a chemical reaction mechanism generated for these fuel blends with about 1500 species and 27 500 reactions and underline the superiority of this approach with the argument that fuels with identical octane numbers could show distinctly different ignition kinetics in modern engines [43].

While chemical reaction mechanisms predicting combustion behavior and exhaust composition, especially regarding non-regulated species-specific contributions to the HC fraction, are in a reasonable state of development for conventional petroleum-based hydrocarbon fuels [28–32] and their application in conventional engines, advanced engine concepts using low-temperature reactions [44–47] and biofuels or biofuel–hydrocarbon mixtures [38, 40, 48–53] add chemical complexity. Further chemical problems related to the respective fuel–engine system can be mentioned only in passing here, namely concepts for highly efficient exhaust gas after treatment [54–56]. As for the combustion process itself, the complex gas-phase and heterogeneous reactions involved in catalytic reduction and/or oxidation of combustion engine exhaust species depend on a large number of physico-chemical and engineering parameters, and development and improvement must rely again on fundamental understanding of the reaction mechanisms as a function of the conditions.

To examine the developed models with respect to their suitability, in short, to "validate" their performance, measurements are needed that can critically inspect and assess the reaction processes from the lab scale to the engine. Under practically relevant conditions, optical methods, often employing lasers, are advantageous since they can measure certain crucial quantities related to, e.g. mixture formation, heat release, and emissions [57–59]. Numerous techniques exist that can be used individually or in combination. With respect to the detailed chemical reaction behavior, however, it is often highly useful to decouple aspects of the harsher

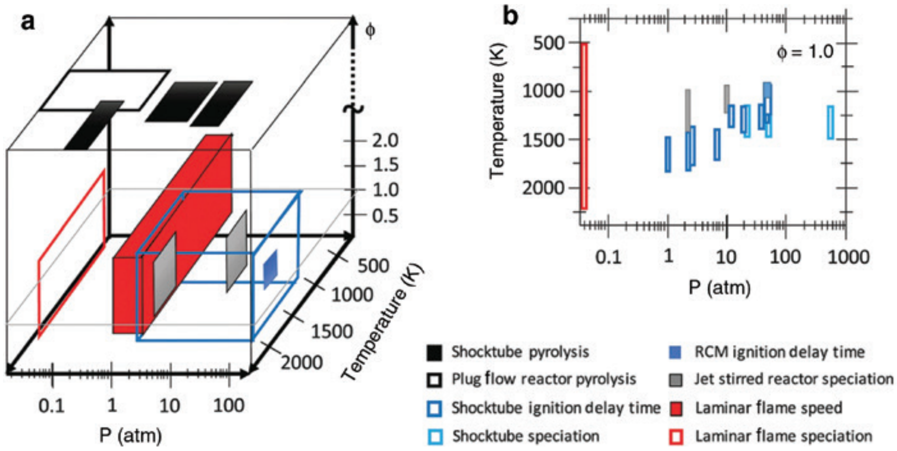

Fig. 4: Overview of the experimental data in the literature for toluene pyrolysis and oxidation. Reprinted from Fig. 2 in Ref. [72] with permission by the Royal Society of Chemistry. (a) three-dimensional diagram of experimental data as a function of temperature, pressure and stoichiometry; (b) two-dimensional plot at $\phi = 1.0$.

conditions of the application, such as turbulent flow, flame–wall interactions, high pressure, presence of more than one phase including droplets, sprays, and particles, from the fuel-specific chemistry in question. Chemical combustion research under laminar conditions in shock tubes, rapid compression machines (RCMs), flames, and plug flow reactors (PFRs), as well as in jet-stirred reactors (JSRs) can cover key aspects of the combustion process, including more global parameters such as laminar flame speed and ignition delay times, or a more detailed set of species concentrations, often as a function of reaction progress [60–62]. Recent examples of such detailed diagnostics are devoted to some of the most complex chemical problems in combustion regarding the detection of many fuel-specific labile species in the low-temperature regime [46, 63–65] as well as the formation of emergent to mature soot particles and their high-molecular-weight precursors [66–70].

Comprehensive model validation strategies make use of many available experimental data obtained under different reaction conditions [71, 72]. The example in Fig. 4 demonstrates the situation for toluene pyrolysis and oxidation [72]; toluene as an alkylated aromatic reference species can represent the behavior of such components in surrogate mixtures for realistic fuels. With RON = 120, toluene can be found in the extended range for alkylated aromatics discussed in Fig. 3. The three-dimensional diagram in Fig. 4a provides the existing experimental data as a function of the most relevant quantities temperature, pressure, and equivalence ratio ϕ, a measure of the stoichiometry of the fuel–air mixture. In the given parameter space, it is evident that typical experimental set-ups each cover only certain ranges of practical interest, and that especially below about 1000 K, in the important LTC regime, experimental data is unavailable, as particularly evident in Fig. 4b. It is thus not surprising that existing models, considering this lack of experimental validation targets, are found to exhibit large differences and uncertainties in this range, with about two orders of magnitude discrepancies in the prediction of toluene ignition delay time at 20 bar and 800 K [72]. Such comprehensive analyses can guide both experimental and theoretical developments aiming at a better understanding of the low-temperature reactions of this important class of fuel components.

Examples: understanding fuel-specific chemistry

The demand for deeper understanding of the performance of real-world combustion applications, including important aspects such as their ignition and emission behavior, has motivated a large number of recent investigations, combining efforts of theoretical chemists, experimentalists, modelers, and engineers. The systematic development and validation of fundamental, detailed combustion kinetics is progressing from the C_0–C_4 range of fuels towards larger hydrocarbons and oxygenates, striving for correct representation of single rate expressions on the one side [72, 73] and inclusive, large reaction mechanisms on the other [17, 31, 32, 35, 47, 48]. Specific effort has been devoted recently to hydrocarbon and oxygenated C_5 fuels such as pentanes [74–79], pentenes [77, 79–82], pentanols [83, 84], and pentanones [85–87]. Fuels that may be accessible from cellulosic biomass including higher alcohols [48, 88] and furan derivatives [40, 89] have been studied because of their attractive combustion-related properties, energy content, and favorable particulate emission reductions. Because of the importance of the ester functional group in biodiesel, molecular-structure-dependent combustion reactions of small methyl and ethyl esters are the subject of intense recent research [90–95], similar to those of compounds such as ethyl levulinate that may be derived from cellulosic biomass [96]. The large variety of oxygenated fuels with different molecular sizes and structures demands careful consideration – among other relevant properties – of energy density (suggesting larger fuel molecules with low oxygen content) and low emissions of potentially harmful or toxic oxygenated compounds (suggesting structurally simple, typically smaller fuel molecules). Further aspects to be considered should include the sustainable and energy-efficient production of the respective fuels in addition to their performance in practical combustion systems.

Ether fuels

A particularly interesting class of oxygenated fuels, for which detailed combustion mechanisms exist or are being developed with emphasis on the low-temperature regime, includes ethers such as dimethyl ether (DME) [71, 97], diethyl ether (DEE) [98–100], and di-*n*-butylether (DBE) [101–103]. In hydrocarbon–oxygenate mixtures these are typically attractive, also compared to their alcohol isomers [50, 51] with respect to their lower soot precursor formation tendencies. Comparisons among DME, DEE, and DBE under similar flame conditions [103] show that the presence of only C_1 and/or C_2 moieties in the fuel molecule lowers the formation tendency of C_3–C_6 compounds, thus contributing to a reduction of soot precursor concentrations.

Especially oligomeric oxymethylene ethers (OMEs) [104–107] receive large interest as potentially clean fuels. They constitute a group of compounds that feature only C_1 carbon blocks joined by ether functional groups with the general formula of $CH_3O(CH_2O)_nCH_3$. For practical purposes, members of this family in the range $n=1$–5 are suggested, of which mainly the representatives with $n=1$, called OME_1, dimethoxymethane (DMM), or methylal, [52, 108–110], and OME_3 with $n=3$ [111] have been studied with regard to their combustion properties and mechanisms. DME can be regarded as a compound with $n=0$ in this series. These compounds are being discussed as potential additives or diesel replacement fuels and can be produced from different fossil and biogenic feedstocks. Their synthesis and physico-chemical properties [104] as well as their combustion behavior in single-cylinder research engines have been recently examined [105, 107], including also a lifecycle assessment for their production from different woody biomass sources [106]. Attempts to understand their attractive combustion properties that may lead to large reductions in soot while avoiding increasing NO_x emissions [105, 107] have only started very recently. The example of OMEs is therefore well suited to illustrate the combined advances that can be expected from theory, model development, laboratory experiments, and engine measurements.

The initial destruction of the fuel molecule occurs typically by H-abstraction reactions to form fuel radicals that then react further by oxygen addition or β-scission reactions. Chain-branching reactions are an important factor for temperature-dependent reactivity [108, 109]. Branching ratios between different reaction channels, e.g. those determining the partition between different early isomeric intermediates, and the further competing reactions of these early products as a function of temperature, pressure, and stoichiometry are instrumental for the subsequent reaction pathways. It is thus important for the development of chemical reaction models to predict these first steps correctly.

Kopp et al. [110] have recently stressed that much of the earlier mechanisms for OME combustion have included kinetics derived by analogy from DME or DEE oxidation. The molecular structure of DME and DEE, however, contains neither the $O–CH_2–O$ group characteristic of the OME structure, nor the $O–(CH–O)–O$ sequence formed in intermediates of OME oxidation; the authors have therefore addressed their influence in the reaction pathways for OMEs. Since such structures are labile and not easily investigated experimentally, Kopp et al. [110] have determined important thermochemical quantities such as enthalpies, entropies, and heat capacities as well as crucial rate coefficients for these reactions using high-level computational methods.

Figure 5 shows, as one result from their study, the potential energy surface for important DMM reactions [110]. The fuel molecule (middle) is seen to form two fuel radicals, namely by H-abstraction from the two terminal CH_3 groups (R1, shown left), and from the central carbon (R3, right). Entropic and bond energy effects both influence the branching ratio. The fuel radicals will not isomerize because of the large energy barrier that separates them but will undergo oxygen addition and β-scission reactions. The diagram shows, in addition to the formation of several highly oxygenated ROO intermediates, the easy access to formaldehyde, CH_2O (via R1 and the related transition state TS) and methyl radical, CH_3 (via R3, TS) [110].

These results are now available for improving the fundamental basis for more accurate and reliable kinetic model development [110]. Vermeire et al. [109] and Sun et al. [108] have recently studied the low-temperature reaction pathways during DMM oxidation experimentally. Both investigations have been conducted in jet-stirred reactors and have provided temperature-dependent species profiles determined with combinations of advanced analytic methods; Sun et al. [108] have also varied the pressure. In contrast to DME (OME_0), DMM (OME_1) was not seen to exhibit a similarly significant low-temperature reactivity. Sun et al. [108] discuss this behavior that depends also on the chosen equivalence ratio in terms of the branching ratio and competition of the oxidation and scission reactions of the dominant fuel radical. Their newly developed model that does, however, not yet include the contributions of Kopp et al. [110], represents their own experimental results and the slightly earlier ones from Vermeire et al. [109] quite well. Since also the latter study [109] offers a new model that includes newly calculated potential energy surfaces and kinetic coefficients for a number of low-temperature reactions, especially of important radicals, and finds the model in reasonable agreement with their experiments, it is evident that within only about a half year between these three publications, substantial progress has been made in model development that can explain the reactivity and most of the observed intermediates.

Figure 6 shows a rate of production analysis for DMM oxidation performed with the model of Ref. [109] at two different conditions. The formation of the two fuel radicals discussed earlier is seen to depend on the conditions; the dominant pathway here proceeds through the H-abstraction at the central carbon, with subsequent scission to yield methyl and methyl formate. Due to a low barrier this reaction proceeds fast, and the initially dominant radical has a too short lifetime for the competing oxygen addition, thus not supporting the chain branching reactions needed to enhance the reactivity [109]. Methyl formate is not consumed significantly further under these conditions and has also been observed as a product in premixed DMM-doped *n*-heptane flames [52].

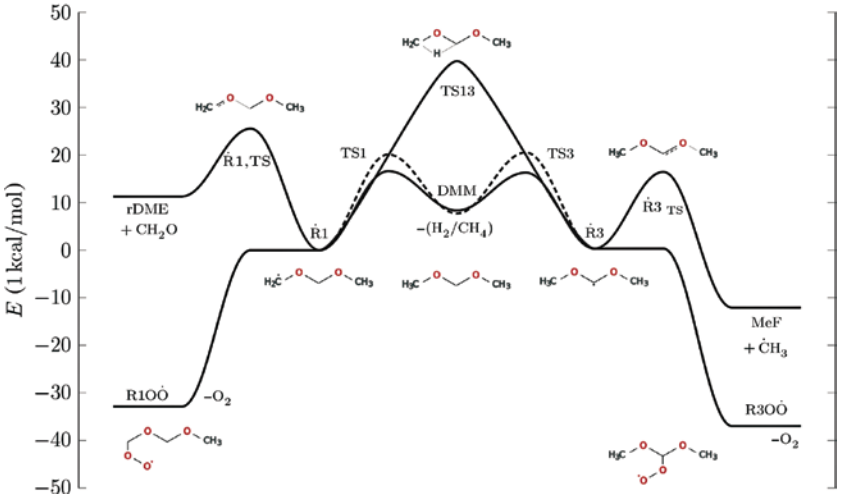

Fig. 5: Potential energy surface for important reactions of dimethoxymethane (DMM); for details see the original publication. Reprinted from Fig. 1 in Ref. [110] with permission by Elsevier/The Combustion Institute.

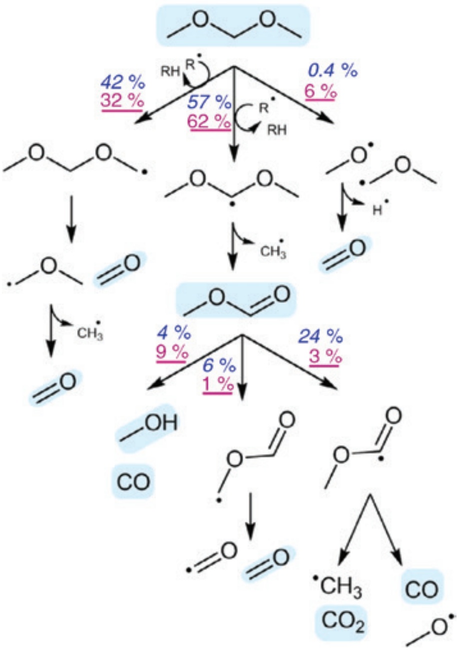

Fig. 6: Rate of production analysis to identify important pathways during low-temperature oxidation of dimethoxymethane (DMM). Rate of productions relative to the consumption of DMM are presented at stoichiometric conditions at 650 K (blue, italic) and 700 K (red, underlined). Reprinted from Fig. 10 of Ref. [109] with permission by Elsevier/The Combustion Institute.

Omari et al. [107] have recently investigated the addition of OME_1 (DMM) to regular diesel fuel in the range of 0–80 % in a single-cylinder research engine. To identify the optimal blending ratio, they have considered different load points (LP) at pre-defined NO_x emissions and determined the soot reduction potential with increasing OME_1 addition (given as OME_1 content in vol%) while monitoring important fuel blend properties. The results for two operating points (LP3 and LP4), with different set NO_x levels, are presented in Fig. 7 that shows the particulate matter (PM) and the cetane number (CN) as a function of heating value, oxygen content, and OME_1 fraction [107]. Up to about 40 % OME_1 content in diesel leads to high PM reduction, but higher OME_1 content affects the heating value and cetane number without much further effect on PM emissions. Considering reasonable limits in CN and heating value, a blend with 35 % OME_1 in diesel fuel was selected which can achieve a soot reduction of ~90 % with only 10 % and 15 % decrease in CN and heating value, respectively [107].

With the OME_1 blend, the unfavorable soot–NO_x tradeoff problem – a severe limitation for achieving cleaner conventional diesel propulsion – could be avoided completely [107]. Härtl et al. [105] have reported similar observations. Several factors contribute to the favorable performance of diesel–OME_1 blends [105, 107] that are not a mere result of the oxygen content of the molecule, also compared to other oxygenates [105]. The chemical structure without C–C bonds effectively suppresses the typical build-up reactions towards soot precursors, PAHs, and eventually, soot, since compounds with high carbon content are not easily formed. Although with a CN of 24 [107], OME_1 is not well suited as a pure fuel, it is well miscible with diesel fuel, and mixtures can tolerate a high level of exhaust gas recirculation needed for keeping appropriate NO_x levels below e.g. Euro VI (EU6d) limits [105, 107]. OME_1 with its high volatility also supports fast evaporation and efficient mixing, leading to a more premixed character of the combustion that can contribute to avoiding high local temperatures that would lead to increased NO_x formation [107]. Härtl et al. [105] also examined the HC composition upon OME_1 use in their research engine by FTIR spectrometry, with particular attention to formaldehyde and methane as easily formed intermediates in the fuel destruction reactions. CH_2O levels were below their detection limit, while methane made up almost all of HC, depending on the respective stoichiometry [105].

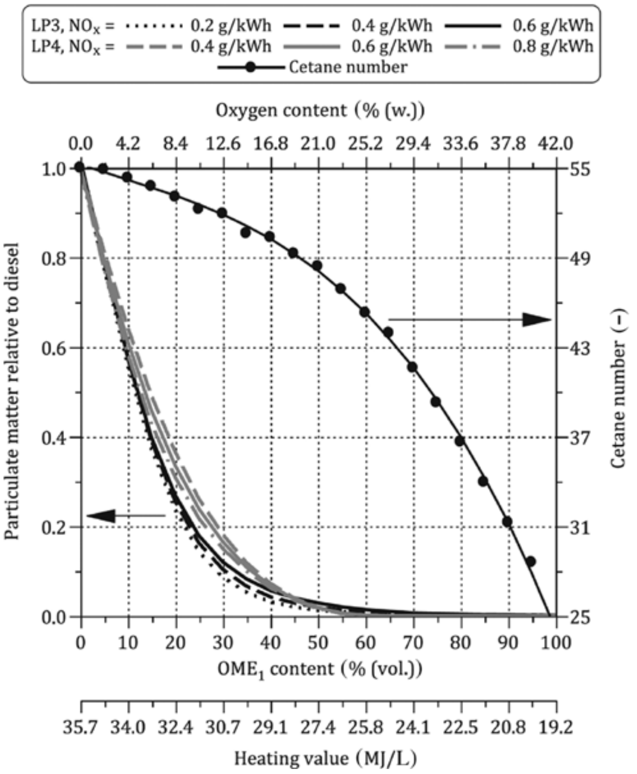

Fig. 7: Modeled reduction of particulate matter relative to diesel fuel as function of the content of OME_1 in the blend at two different operating conditions, LP3 and LP4. Reprinted from Fig. 10 in [107] with permission by Elsevier.

Omari et al. [107] discuss potential future production of oxymethylene ethers from water and methanol obtained using CO_2 from carbon dioxide capture and sustainable H_2. As an attractive fuel additive with superior emission and reasonable combustion characteristics, it might be one route to contribute to cleaner diesel-like propulsion concepts in the future. Partial diesel fuel replacement with OMEs could also serve to improve the carbon balance.

While progress is being made regarding promising fuels and chemical understanding of their design and use in advanced engines, many details of combustion mechanisms need further intense inspection, particularly under practically relevant conditions. Fundamental research in laboratory set-ups can contribute to such advances by providing experimental data for model validation in systems that have not been studied in depth previously. Two examples will be discussed to illustrate selected developments, the first devoted to interactive effects in fuel mixtures of hydrocarbon and oxygenated components, and the second to soot nucleation.

Hydrocarbon-oxygenate fuel blends

Interactive effects between the reactive intermediates formed from different fuel components can be of influence particularly in the LTC regime, where they affect ignition, and for the formation of soot precursors, PAHs, and soot, where the joint pool of reactive species might enhance certain reaction pathways that build up larger molecules and carbon structures. The comprehensive, recent article of Sarathy et al. [35] gives an overview of numerous combustion experiments and modeling activities for gasoline surrogates, including a few oxygenated additives, and focuses mainly on ignition delay times and laminar flame speeds. Detailed interactive effects on ignition delay times were, for example, reported by Burke et al. [112] for mixtures of the structurally simple fuels methane and DME, the former as the main component of natural gas and the latter as a biogenic substituent or fuel additive. Results were provided from shock tube and RCM experiments in the range of 600–1600 K and 7–41 bar relevant for gas turbine combustion conditions. Their analysis with a well-validated model for the two fuels shows that DME dominates the ignition characteristics in the mixtures, even if methane is the more abundant component: with even small amounts of DME, the formation of decisive radicals can occur already at lower temperatures, and as a function of temperature, chain-branching reactions and H-abstraction reactions contribute to increase the rate of methane combustion [112].

Speciation information, i.e. extensive sets of quantitative intermediate species concentration profiles for a given fuel combination as a function of reaction time or temperature, provide even stricter conditions for the examination of reaction model performance than more global combustion parameters such as ignition delay times. Detailed investigations for combinations of hydrocarbon and biogenic fuel components have only recently found higher attention. Such detailed experimental speciation data for selected binary hydrocarbon-oxygenate mixtures have been reported from JSR studies, for example by Dagaut and Togbé [113] for mixtures of ethanol (as a biofuel that is in use today) and *n*-heptane (an automotive reference fuel) in the range of 500–1070 K at ~10 bar. The authors note that such investigations of the co-oxidation of hydrocarbons and ethanol were not performed before their study. Their experiment provided temperature-dependent mole fractions for major species and selected stable intermediates for different conditions and analyzed the reaction pathways with a combined model for both constituents. Not unexpectedly, increasing ethanol addition favored the formation of acetaldehyde that can contribute to harmful automobile emissions [113].

Particularly valuable results can be obtained from the systematic variation of the fuel structure motives (e.g. saturation and branching degree) in studies of hydrocarbon–oxygenate fuel mixtures, as reported for the oxidation of hydrocarbon base fuels of different chain length, blended with ethers, alcohols, or esters [50–53, 114]. Interactive effects have been observed in particular in the low-temperature reactivity for mixtures of *n*-pentane with DME or ethanol as reported by Jin et al. [51]. In their investigation in a laminar flow reactor, the authors have compared the temperature-dependent mole fraction profiles for a large number of species with two established literature models that can represent all three fuels. Figure 8 presents mole fraction maxima for selected oxygenated (left panels) and hydrocarbon (right panels) intermediates for five mixture conditions (lines). All profiles are normalized by the inlet mole fraction of *n*-pentane, so that all lines would fall on top of each other if there were no interactive effects (please note the logarithmic scale). The top row shows the experimental results from mass spectrometric analysis, presenting such interactive chemistry between the two fuel compounds especially for some of the oxygenated intermediates. Counteracting effects of DME versus ethanol addition to *n*-pentane under identical conditions are seen in some cases (e.g. for $C_2H_4O_2$ calibrated as acetic acid) that underline the influence of fuel-structure-specific reactions for the two oxygenated isomers. Striking differences are seen in Fig. 8 not only between experimental and modeling results, but also between the two used models by Bugler et al. [74, 75] (middle row) and Ranzi et al. [47] (bottom row), suggesting that the joint low-temperature oxidation chemistry of these three fuels should be carefully re-evaluated and may need improvement.

Soot nucleation

To address a partly unsolved question of eminent fundamental and practical importance, recent work is concerned with the nucleation of soot particles from their high-molecular precursors, the nature of which remains subject of theoretical approaches and, in part, chemical inspiration. Several developments contribute to this recent focus, namely the emission of very small particles in the range of a few nanometers by modern engines, changes of regulations to limit number density rather than mass that favors attention to high fractions of small particles, and the recent accessibility of very small carbon particles to detection with sophisticated in and ex situ methods [66–68, 115, 116]. Because of the adverse effects of soot emission, the combustion community strives to develop complete mechanisms that can describe the entire carbon growth process from the fuel-specific formation of gas-phase intermediates to the mature soot particle [117–120]. Because of the thousands of species involved and the exponential growth of structural isomers with molecular size, such models typically include

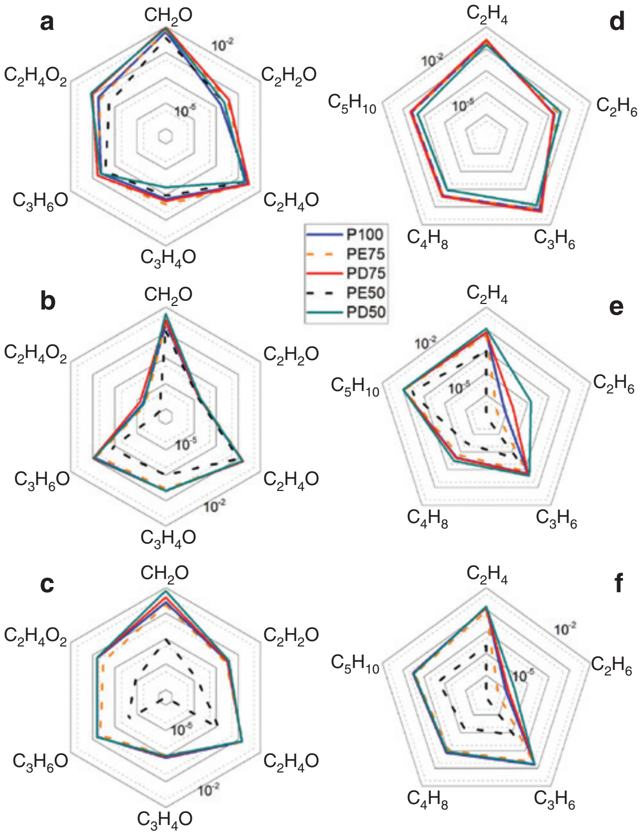

Fig. 8: Mole fractions of selected oxygenated and hydrocarbon intermediates during the oxidation of mixtures (100, 75, and 50 %) of *n*-pentane (P) with DME (D) and/or ethanol (E) at their respective maxima in the low-temperature regime (logarithmic scale); the mole fraction of each species is normalized by the inlet mole fraction of *n*-pentane for the respective condition. (a and d): experimental results; (b and e) predictions with the NUIG model by Bugler et al. [74, 75]; (c and f) predictions with the Polimi model by Ranzi et al. [47]. For details, see original publication. Reprinted from Fig. 14 of Ref. [51] with permission by Elsevier/The Combustion Institute.

and connect different simulation approaches for the smaller molecular precursors, the formation of PAHs, and the nucleation and growth of particles. It is highly difficult to validate such models along the entire growth sequence. Figure 9 presents selected results from a recent study of Kholghy et al. [118]. They have predicted soot mole fractions in a so-called nucleation flame that was investigated experimentally by Desgroux et al. [121] using in situ laser-induced incandescence (LII), online jet-cooled laser-induced fluorescence (JCLIF) and ex situ secondary ion mass spectrometry (ToF-SIMS) to measure important PAH and soot particle concentrations. Kholghy et al. [118] consider not only reversible dimerization of PAHs of different sizes by van der Waals forces, as in earlier Reversible Nucleation (RN) models, but assume subsequent chemical bond formation in their Reversible Nucleation and PAH Chemical Bond Formation (RNCBF) model. By this approach, the authors [118] achieve a much better agreement with the experimental data than the RN model that predicts at least two orders of magnitude lower soot volume fractions (Fig. 9a). The form of the predicted curve with the RNCBF model [118] also matches the experimental observations better than the Irreversible Nucleation (IN) approach [121], as evident from Fig. 9b. Moreover, detailed comparisons with experimental PAH concentration profiles given in [118] show also acceptable performance of the employed base mechanism.

Although the results seem promising, several important questions remain. As one aspect, the predicted curve in Fig. 9b had to be shifted to match the experiment, while reasons for such assumed shifts are unclear. More importantly, however, potential limitations of detecting nanometer-sized incipient soot particles by LII are a subject of current debate [68, 115, 117], awaiting further experimental corroboration and clarification of terminology and properties between nascent, or incipient, and mature soot. It remains to be demonstrated whether

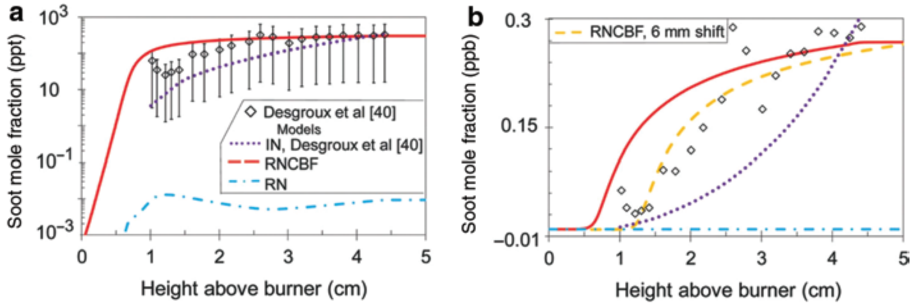

Fig. 9: Comparison of the concentration of incipient soot measured by laser-induced incandescence (LII) with predicted total dimer concentration using, Reversible Nucleation and PAH Chemical Bond Formation (RNCBF), Irreversible Nucleation (IN) and Reversible Nucleation (RN) models in (a) log scale and (b) linear scale. (Note that for the LII experiment and IN model, the cited literature in the left graph pertains to the reference in the original publication). Reprinted from Fig. 7 in Ref. [118], with permission by the Royal Society of Chemistry.

initial experiments using coherent femtosecond X-ray free-electron laser pulses, that from combined diffraction and mass spectrometric measurements could successfully demonstrate in situ analysis of the morphology and further characteristics of individual spark-generated sub-micrometer soot particles [122] will develop into a tool that could also be applied to detect and characterize nucleating soot in its flame environment. As the carbon structures just before particle nucleation are not amenable to current analytic methods, insight from theory regarding, for example, rate coefficients for important reactions involved in or following dimerization could prove useful. Since appreciable numbers of small soot particles can contribute to harmful emissions from both, modern diesel and gasoline engines [123–125], in-depth fundamental understanding is urgently awaited.

Perspectives

Chemical issues with today's fuels, combustion engines, and their emissions induce discussions about clean transportation in the future. Guidance is needed but not easy considering various technical factors on the one hand, such as energy density and range (see Fig. 1), production processes, delivery, and infrastructure, and further factors such as consumer preferences, economic, and environmental concerns as well as legislative directions on the other.

Regarding existing technologies, Orsi et al. [14] have performed a multi-dimensional comparison of passenger vehicles with respect to their CO_2 emissions, petroleum consumption, and fuel cost. Among the various fuel and propulsion concepts considered, they found no clear winner with regard to these three parameters. Reduced CO_2 could potentially be achieved with biofuel addition and with electric vehicles (EVs) using low-carbon electricity, at increased costs, however. According to their evaluation, compressed natural gas is competitive economically and with respect to petroleum consumption, but not in terms of CO_2 emissions, while partial electrification in hybrids leads to opposite performance trends [14]. They conclude that a sudden transition away from gasoline and diesel fuels for passenger cars is unlikely, but identify hybrid electric vehicles (HEVs) as a short-term bridge technology towards more sustainable long-term solutions that may be regionally different [14].

In their life-cycle analysis with a focus on efficient and clean vehicle solutions for China, Wang et al. [13] conclude that EVs as well as fuel cell vehicles (FCVs) powered with electrolysis-generated hydrogen will for some time into the future cause more environmental problems than vehicles using internal combustion engines as consequence of the coal-dominated electricity in China, and they advise that low-carbon electricity should be available before large-scale introduction of such EV and FCV propulsion concepts. While FCVs using natural gas reforming are less dependent on the present energy mix, their performance was not seen to be superior to that of modern combustion engines in their assessment considering well-to-wheels efficiency, energy consumption, carbon, and especially, associated particulate emissions [13].

It is instructive to look at the examples on the scale of potential transformations needed given in the recent perspective by Kalghatgi [126], where he compares the estimated present fuel use *per day* of about 4.8 billion liters each of gasoline and diesel, plus 1.3 billion liters of jet fuel, representing a global need of transportation energy of about 105 TWh *per day*, with the global consumption of solar and wind energy of 1292 TWh *in the entire year* 2016. Although some strategies advocate battery electric vehicles (BEVs) to (partially) replace combustion engines, aspects to be considered include the already discussed need for low-carbon electricity [13, 14] that is unlikely to be available in the necessary extent in many parts of the world for the next decades [126]. Apart from environmental and geopolitical issues regarding (current) batteries and the materials involved for their production [13, 126], technical considerations include a (potentially unrealistic) high-capacity charging infrastructure, competitive charging duration, and charging patterns adapted to consumer needs that are not easily met with fluctuating energy sources without appropriate storage; also, the carbon signature of the battery production itself must be considered [126]. Alternatives including fuels such as liquid petroleum gas (LPG) or compressed natural gas (CNG) will not ultimately lead to carbon-free transportation, whereas for FCVs using hydrogen, carbon-free production, on-board storage, and distribution infrastructure as well as the associated significant costs are problems that are unlikely to be solved short-term [126]. In comparison, HEVs with their much smaller batteries (powered by the combustion engine) and clean combustion engines using, for example, reactivity-controlled low-temperature strategies, are seen as a highly competitive, (at least) mid-term alternative [126].

Regarding one perspective of clean propulsion that could potentially circumvent some of the challenges discussed above, discussions include hydrogen-rich energy vectors such as, for example, ammonia [127–132]. Briefly, among other options for a future hydrogen economy, ammonia – as a carbon-free small molecule – represents a versatile chemical for flexible use as a fuel in internal combustion engines and fuel cells as well as a thermochemical working fluid as, e.g. in cooling or heating systems [127, 128, 130]. Similar to hydrogen, it can be produced from fossil sources, biomass, and (renewable) electricity. While its end use is CO_2-free, its carbon signature depends on its production route [127, 128]. Towards its advantages count also well-established large-scale production, transportation, and storage infrastructures that make it attractive as a direct fuel or in mixtures with, for example, methane [131, 133] or hydrogen [134], and as a (potentially on-board) hydrogen source [129, 130]. Intensified research is devoted to improving the efficient and economic thermal cracking of NH_3 to release hydrogen [129], and to understand the combustion characteristics and reaction mechanisms of ammonia under practical conditions, as e.g. relevant for gas turbine combustors [131]. Challenges include the low burning velocity of NH_3, its toxicity, and the formation of NO_x from the nitrogen in the molecule, which can be controlled, however, with existing technology, also recognizing that NH_3 is a NO_x reducing agent [127, 131]. Since ammonia also acts as a coolant, it can furthermore contribute to a favorable engine heat management and associated efficiency gains [127]. Combustion of ammonia has been described to be a potential option for power generation [133] as well as air transportation [132], but its performance remains to be seen in comparison to existing technologies [135].

Regarding future opportunities, it is useful to remember that combustion is one, but not the only, important building block in the energy transformation, and that large-scale economic, sustainable transportation has many facets – and not yet one preferable option – that should be considered [1, 15, 136]. Understanding the relevant chemistry is a cornerstone in the choice of fuels and energy storage media that may be useful for systems integration. Recent work on on-board fuel reforming [137], on using IC engines in polygeneration processes for the production of higher-value chemicals [138, 139], as an approach for energy conversion and storage [139, 140], as well as on co-generation of power and syngas [141] might serve as indications for future opportunities.

It should not be neglected, however, that consumer behavior is another factor. Brunner et al. [142] have recently analyzed several urban transportation options, and one result of their study is given in Fig. 10. Here, the equivalent fuel consumption per person in the vehicle is compared according to a calculated traffic weight indicator specified in the original paper [142] for a number of current ground transportation possibilities.

It comes to no surprise that human-powered transportation modes (pedestrian, bicycle) and sports utility vehicles (SUVs) are found at opposite ends of this performance evaluation. The authors note that electric

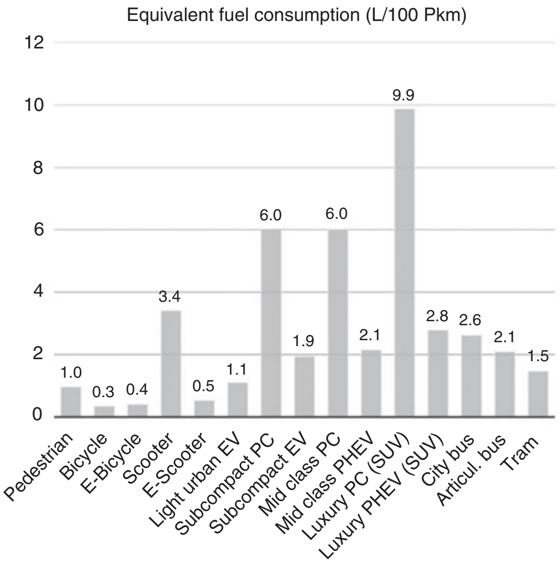

Fig. 10: Equivalent fuel consumption per person (P) (in L/100 Pkm) in the vehicle (EV: electric vehicle, PC: passenger car, PHEV: plug-in hybrid electric vehicle, SUV: sports utility vehicle). Reprinted (with color adapted) from Fig. 6 (right) in Ref. [142], SpringerOpen articles. For details on evaluation criteria and methodology, see original publication.

scooters and light EVs count among the least fuel-consuming options for urban mobility, and can be competitive regarding this criterion with public transportation [142]. Nevertheless, any unnecessary mile driven, directly, i.e. by the consumer or indirectly, e.g. for transporting consumer goods, or any kilometer covered with an inadequate choice of vehicle increases the resulting global problems. Time for changes is short, as discussed by Anderson and Clapp [143] from a perspective of climate change. It cannot be overemphasized, that – as stated by the French President addressing the US congress on April 25, 2018 – “there is no Planet B” [144].

Acknowledgements: The author wishes to acknowledge partial support of her work by the Deutsche Forschungsgemeinschaft (Funder Id: 10.13039/501100001659) within the Research Unit FOR 2401, “Optimization-Based Multiscale Control of Low-Temperature Engine Concepts”. She is also grateful for careful reading by Andreas Brockhinke, Lena Ruwe, Steffen Schmitt, and Julia Wullenkord, Bielefeld, Germany; as well as by Christof Schulz, Duisburg, Germany; Luc-Sy Tran, Lille, France; and Hai Wang, Stanford, USA.

Article note: A special collection of invited papers by recipients of the IUPAC Distinguished Women in Chemistry and Chemical Engineering Awards.

References

[1] F. Ausfelder, C. Beilmann, M. Bertau, S. Bräuninger, A. Heinzel, R. Hoer, W. Koch, F. Mahlendorf, A. Metzelthin, M. Peuckert, L. Plass, K. Räuchle, M. Reuter, G. Schaub, S. Schiebahn, E. Schwab, F. Schüth, D. Stolten, G. Teßmer, K. Wagemann, K.-F. Ziegahn. *ChemBioEng. Rev.* **4**, 144 (2017).
[2] A. Varone, M. Ferrari. *Ren. Sust. Energy Rev.* **45**, 207 (2015).
[3] A. B. Gallo, J. R. Simões-Moreira, H. K. M. Costa, M. M. Santos, E. Moutinho dos Santos. *Renew. Sustain. Energy Rev.* **65**, 800 (2016).
[4] T. J. Wallington, J. E. Anderson, D. J. Siegel, M. A. Tamor, S. A. Mueller, S. L. Winkler, O. J. Nielsen. *J. Chem. Educ.* **90**, 440 (2013).
[5] *BP Energy Outlook 2018 Edition*, available under www.bp.com, accessed May 01, 2018.
[6] S. C. Davis, S. E. Williams, R. G. Boundy. *Transportation Energy Data Book*, Edition 36, Oak Ridge National Laboratory, Oak Ridge, TN, USA, prepared for the U.S. Department of Energy, October 2017, available under cta.ornl.gov, accessed April 30, 2018.

[7] Intergovernmental Panel on Climate Change, *Climate Change 2014: Synthesis Report. Contribution of Working Groups I, II and III to the Fifth Assessment Report of the Intergovernmental Panel on Climate Change* [Core Writing Team, R.K. Pachauri and L.A. Meyer (eds.)]. IPCC, Geneva, Switzerland, pp. 151, available under www.ipcc.ch, accessed May 02, 2018.

[8] International Energy Agency, *World Energy Outlook Special Report: Energy and Climate Change*, 2015, available under www.iea.org, accessed May 02, 2018.

[9] S. S. Lim, T. Vos, A. D. Flaxman, G. Danaei, K. Shibuya, H. Adair-Rohani, et al. (including about 200 further authors). *Lancet* **380**, 2224 (2012).

[10] T. C. Bond, S. J. Doherty, D. W. Fahey, P. M. Forster, T. Berntsen, B. J. DeAngelo, M. G. Flanner, S. Ghan, B. Kärcher, D. Koch, S. Kinne, Y. Kondo, P. K. Quinn, M. C. Sarofim, M. G. Schultz, M. Schulz, C. Venkataraman, H. Zhang, S. Zhang, N. Bellouin, S. K. Guttikunda, P. K. Hopke, M. Z. Jacobson, J. W. Kaiser, Z. Klimont, U. Lohmann, J. P. Schwarz, D. Shindell, T. Storelvmo, S. G. Warren, C. S. Zender. *J. Geophys. Res. Atmos.* **118**, 5380 (2013).

[11] Y. Zhu, L. Huang, J. Li, Q. Ying, H. Zhang, X. Liu, H. Liao, N. Li, Z. Liu, Y. Mao, H. Fang, J. Hu. *Environ. Intern.* **115**, 343 (2018).

[12] A. K. Agarwal, A. P. Singh, R. K. Maurya. *Prog. Energy Combust. Sci.* **61**, 1 (2017) and literature therein.

[13] D. Wang, N. Zamel, K. Jiao, Y. Zhou, S. Yu, Q. Du, Y. Yin. *Energy* **59**, 402 (2013).

[14] F. Orsi, M. Muratori, M. Rocco, E. Colombo, G. Rizzoni. *Appl. Energy* **169**, 197 (2016).

[15] M. A. Mac Kinnon, J. Brouwer, S. Samuelsen. *Prog. Energy Combust. Sci.* **64**, 62 (2018).

[16] M. Romero, A. P. de Madrid, C. Mañoso, V. Milanés. *ISA Trans.* **57**, 373 (2015).

[17] H. Wang, R. Xu, K. Wang, C. T. Bowman, R. K. Hanson, D. F. Davidson, K. Brezinsky, F. N. Egolfopoulos. *Combust. Flame* **193**, 502 (2018).

[18] S. M. Sarathy, C. K. Westbrook, M. Mehl, W. J. Pitz, C. Togbe, P. Dagaut, H. Wang, M. A. Oehlschlaeger, U. Niemann, K. Seshadri, P. S. Veloo, C. Ji, F. N. Egolfopoulos, T. Lu. *Combust. Flame* **158**, 2338 (2011).

[19] J. A. Miller, C. T. Bowman. *Prog. Energy Combust. Sci.* **15**, 287 (1989).

[20] P. Glarborg, J. A. Miller, B. Ruscic, S. J. Klippenstein. *Prog. Energy Combust. Sci.* **67**, 31 (2018).

[21] K.-H. Homann. *Angew. Chem. Int. Ed.* **37**, 2434 (1998).

[22] H. Richter, J. B. Howard. *Prog. Energy Combust. Sci.* **26**, 565 (2000).

[23] M. Frenklach. *Phys. Chem. Chem. Phys.* **4**, 2028 (2002).

[24] C. S. McEnally, L. D. Pfefferle, B. Atakan, K. Kohse-Höinghaus. *Prog. Energy Combust. Sci.* **32**, 247 (2006).

[25] B. S. Haynes, H. G. Wagner. *Prog. Energy Combust. Sci.* **7**, 229 (1981).

[26] H. Wang. *Proc. Combust. Inst.* **33**, 41 (2011).

[27] D. D. Das, P. C. St. John, C. S. McEnally, S. Kim, L. D. Pfefferle. *Combust. Flame* **190**, 349 (2018).

[28] C. K. Westbrook, M. Sjöberg, N. P. Cernansky. *Combust. Flame* **195**, 50 (2018), https://doi.org/10.1016/j.combustflame.2018.03.038.

[29] D. Healy, D. M. Kalitan, C. J. Aul, E. L. Petersen, G. Bourque, H. J. Curran. *Energy Fuels* **24**, 1521 (2010).

[30] M. Mehl, W. J. Pitz, C. K. Westbrook, H. J. Curran. *Proc. Combust. Inst.* **33**, 193 (2011).

[31] R. Xu, K. Wang, S. Banerjee, J. Shao, T. Parise, Y. Zhu, S. Wang, A. Movaghar, D. J. Lee, R. Zhao, X. Han, Y. Gao, T. Lu, K. Brezinsky, F. N. Egolfopoulos, D. F. Davidson, R. K. Hanson, C. T. Bowman, H. Wang. *Combust. Flame* **193**, 520 (2018).

[32] C. K. Westbrook, M. Mehl, W. J. Pitz, G. Kukkadapu, S. Wagnon, K. Zhang. *Phys. Chem. Chem. Phys.* **20**, 10588 (2018).

[33] P. B. Govindaraju, M. Ihme. *Combust. Flame* **188**, 337 (2018).

[34] L. Cai, H. Pitsch. *Combust. Flame* **162**, 1623 (2015).

[35] S. M. Sarathy, A. Farooq, G. T. Kalghatgi. *Prog. Energy Combust. Sci.* **65**, 67 (2018).

[36] M. D. Boot, M. Tian, E. J. M. Hensen, S. M. Sarathy. *Prog. Energy Combust. Sci.* **60**, 1 (2017).

[37] G. Fontaras, G. Karavalakis, M. Kousoulidou, L. Ntziachristos, E. Bakeas, S. Stournas, Z. Samaras. *Environ. Pollut.* **158**, 2496 (2010).

[38] K. Kohse-Höinghaus, P. Oßwald, T. A. Cool, T. Kasper, N. Hansen, F. Qi, C. K. Westbrook, P. R. Westmoreland. *Angew. Chem. Int. Ed.* **49**, 3572 (2010).

[39] R. Daniel, L. Wei, H. Xu, C. Wang, M. L. Wyszynski, S. Shuai. *Energy Fuels* **26**, 6661 (2012).

[40] W. Leitner, J. Klankermayer, S. Pischinger, H. Pitsch, K. Kohse-Höinghaus. *Angew. Chem. Int. Ed.* **56**, 5412 (2017).

[41] B. Rochette, F. Collin-Bastiani, L. Gicquel, O. Vermorel, D. Veynante, T. Poinsot. *Combust. Flame* **191**, 417 (2018).

[42] K. Kohse-Höinghaus. *Prog. Energy Combust. Sci.* **65**, 1 (2018).

[43] P. Zhang, N. W. Yee, S. V. Filip, C. E. Hetrick, B. Yang, W. H. Green. *Phys. Chem. Chem. Phys.* **20**, 10637 (2018).

[44] F. Battin-Leclerc. *Prog. Energy Combust. Sci.* **34**, 440 (2008).

[45] J. Zádor, C. A. Taatjes, R. X. Fernandes. *Prog. Energy Combust. Sci.* **37**, 371 (2011).

[46] F. Battin-Leclerc, O. Herbinet, P.-A. Glaude, R. Fournet, Z. Zhou, L. Deng, H. Guo, M. Xie, F. Qi. *Angew. Chem. Int. Ed.* **49**, 3169 (2010).

[47] E. Ranzi, C. Cavallotti, A. Cuoci, A. Frassoldati, M. Pelucchi, T. Faravelli. *Combust. Flame* **162**, 1679 (2015).

[48] S. M. Sarathy, P. Oßwald, N. Hansen, K. Kohse-Höinghaus. *Prog. Energy Combust. Sci.* **44**, 40 (2014).

[49] L. S. Tran, B. Sirjean, P.-A. Glaude, R. Fournet, F. Battin-Leclerc. *Energy* **43**, 4 (2012).

[50] L.-S. Tran, J. Pieper, M. Zeng, Y. Li, X. Zhang, W. Li, I. Graf, F. Qi, K. Kohse-Höinghaus. *Combust. Flame* **175**, 47 (2017).

[51] H. Jin, J. Pieper, C. Hemken, E. Bräuer, L. Ruwe, K. Kohse-Höinghaus. *Combust. Flame* **193**, 36 (2018).

[52] G. Chen, W. Yu, J. Fu, J. Mo, Z. Huang, J. Yang, Z. Wang, H. Jin, F. Qi. *Combust. Flame* **159**, 2324 (2012).
[53] M. Zeng, J. Wullenkord, I. Graf, K. Kohse-Höinghaus. *Combust. Flame* **184**, 41 (2017).
[54] J. Koop, O. Deutschmann. *Appl. Catal. B: Environm.* **91**, 47 (2009).
[55] M. P. Harold. *Curr. Opin. Chem. Eng.* **1**, 303 (2012).
[56] P. S. Metkar, M. P. Harold, V. Balakotaiah. *Chem. Eng. Sci.* **87**, 51 (2013).
[57] R. K. Hanson. *Proc. Combust. Inst.* **33**, 1 (2011).
[58] V. Sick. *Proc. Combust. Inst.* **34**, 3509 (2013).
[59] A. Dreizler, B. Böhm. *Proc. Combust. Inst.* **35**, 37 (2015).
[60] F. N. Egolfopoulos, N. Hansen, Y. Ju, K. Kohse-Höinghaus, C. K. Law, F. Qi. *Prog. Energy Combust. Sci.* **43**, 36 (2014).
[61] F. Qi. *Proc. Combust. Inst.* **34**, 33 (2013).
[62] N. Hansen, T. A. Cool, P. R. Westmoreland, K. Kohse-Höinghaus. *Prog. Energy Combust. Sci.* **35**, 168 (2009).
[63] Z. Wang, D. M. Popolan-Vaida, B. Chen, K. Moshammer, S. Y. Mohamed, H. Wang, S. Sioud, M. A. Raji, K. Kohse-Höinghaus, N. Hansen, P. Dagaut, S. R. Leone, S. M. Sarathy. *Proc. Natl. Acad. Sci.* **114**, 13102 (2017).
[64] A. Rodriguez, O. Herbinet, Z. Wang, F. Qi, C. Fittschen, P. R. Westmoreland, F. Battin-Leclerc. *Proc. Combust. Inst.* **36**, 333 (2017).
[65] K. Moshammer, A. W. Jasper, D. M. Popolan-Vaida, A. Lucassen, P. Diévart, H. Selim, A. J. Eskola, C. A. Taatjes, S. R. Leone, S. M. Sarathy, Y. Ju, P. Dagaut, K. Kohse-Höinghaus, N. Hansen. *J. Phys. Chem. A* **119**, 7361 (2015).
[66] H. A. Michelsen. *Proc. Combust. Inst.* **36**, 717 (2017).
[67] H. A. Michelsen, C. Schulz, G. J. Smallwood, S. Will. *Prog. Energy Combust. Sci.* **51**, 2 (2015).
[68] C. Betrancourt, F. Liu, P. Desgroux, X. Mercier, A. Faccinetto, M. Salamanca, L. Ruwe, K. Kohse-Höinghaus, D. Emmrich, A. Beyer, A. Gölzhäuser, T. Tritscher. *Aerosol Sci. Technol.* **51**, 916 (2017).
[69] M. Sirignano, D. Bartos, M. Conturso, M. Dunn, A. D'Anna, A. R. Masri. *Combust. Flame* **176**, 299 (2017).
[70] S. A. Skeen, H. A. Michelsen, K. R. Wilson, D. M. Popolan, A. Violi, N. Hansen. *J. Aerosol Sci.* **58**, 86 (2013).
[71] A. Rodriguez, O. Frottier, O. Herbinet, R. Fournet, R. Bounaceur, C. Fittschen, F. Battin-Leclerc. *J. Phys. Chem. A* **119**, 7905 (2015).
[72] M. Pelucchi, C. Cavallotti, T. Faravelli, S. J. Klippenstein. *Phys. Chem. Chem. Phys.* **20**, 10607 (2018).
[73] R. S. Tranter, P. T. Lynch, J. B. Randazzo, J. P. A. Lockhart, X. Chen, C. F. Goldsmith. *Phys. Chem. Chem. Phys.* **20**, 10826 (2018).
[74] J. Bugler, A. Rodriguez, O. Herbinet, F. Battin-Leclerc, C. Togbé, G. Dayma, P. Dagaut, H. J. Curran. *Proc. Combust. Inst.* **36**, 441 (2017).
[75] J. Bugler, B. Marks, O. Mathieu, R. Archuleta, A. Camou, C. Grégoire, K. A. Heufer, E. L. Petersen, H. J. Curran. *Combust. Flame* **163**, 138 (2016).
[76] K. Yasunaga, H. Yamada, H. Oshita, K. Hattori, Y. Hidaka, H. Curran. *Combust. Flame* **185**, 335 (2017).
[77] Y. Cheng, E. Hu, X. Lu, X. Li, J. Gong, Q. Li, Z. Huang. *Proc. Combust. Inst.* **36**, 1279 (2017).
[78] L. Ye, L. Zhang, F. Qi. *Combust. Flame* **190**, 119 (2018).
[79] L. Ruwe, K. Moshammer, N. Hansen, K. Kohse-Höinghaus. *Phys. Chem. Chem. Phys.* **20**, 10780 (2018).
[80] L. Ruwe, K. Moshammer, N. Hansen, K. Kohse-Höinghaus. *Combust. Flame* **175**, 34 (2017).
[81] C. K. Westbrook, W. J. Pitz, M. Mehl, P.-A. Glaude, O. Herbinet, S. Bax, F. Battin-Leclerc, O. Mathieu, E. L. Petersen, J. Bugler, H. J. Curran. *J. Phys. Chem. A* **119**, 7462 (2015).
[82] N. Hansen, T. Kasper, S. J. Klippenstein, P. R. Westmoreland, M. E. Law, C. A. Taatjes, K. Kohse-Höinghaus, J. Wang, T. A. Cool. *J. Phys. Chem. A* **111**, 4081 (2007).
[83] C. Togbé, F. Halter, F. Foucher, C. Mounaim-Rousselle, P. Dagaut. *Proc. Combust. Inst.* **33**, 367 (2011).
[84] C. Tang, L. Wei, X. Man, J. Zhang, Z. Huang, C. K. Law. *Combust. Flame* **160**, 520 (2013).
[85] Z. Serinyel, N. Chaumeix, G. Black, J. M. Simmie, H. J. Curran. *J. Phys. Chem. A* **114**, 12176 (2010).
[86] E. E. Dames, K.-Y. Lam, D. F. Davidson, R. K. Hanson. *Combust. Flame* **161**, 1135 (2014).
[87] J. Pieper, C. Hemken, R. Büttgen, I. Graf, N. Hansen, K. A. Heufer, K. Kohse-Höinghaus. *Proc. Combust. Inst.* (2018). https://doi.org/10.1016/j.proci.2018.05.039.
[88] B. R. Kumar, S. Saravanan. *Renew. Sustain. Energy Rev.* **60**, 84 (2016).
[89] L.-S. Tran, Z. Wang, H.-H. Carstensen, C. Hemken, F. Battin-Leclerc, K. Kohse-Höinghaus. *Combust. Flame* **181**, 251 (2017).
[90] D. Felsmann, H. Zhao, Q. Wang, I. Graf, T. Tan, X. Yang, E. A. Carter, Y. Ju, K. Kohse-Höinghaus. *Proc. Combust. Inst.* **36**, 543 (2017).
[91] K. Kumar, C.-J. Sung, B. W. Weber, J. A. Bunnell. *Combust. Flame* **188**, 116 (2018).
[92] H. Ning, J. Wu, L. Ma, W. Ren, D. F. Davidson, R. K. Hanson. *Combust. Flame* **184**, 30 (2017).
[93] S. Dooley, F. L. Dryer, B. Yang, J. Wang, T. A. Cool, T. Kasper, N. Hansen. *Combust. Flame* **158**, 732 (2011).
[94] W. Sun, T. Tao, R. Zhang, H. Liao, C. Huang, F. Zhang, X. Zhang, Y. Zhang, B. Yang. *Combust. Flame* **185**, 173 (2017).
[95] Y. Zhai, B. Feng, W. Yuan, C. Ao, L. Zhang. *Combust. Flame* **191**, 160 (2018).
[96] M. K. Ghosh, M. S. Howard, Y. Zhang, K. Djebbi, G. Capriolo, A. Farooq, H. J. Curran, S. Dooley. *Combust. Flame* **193**, 157 (2018).
[97] K. Moshammer, A. W. Jasper, D. M. Popolan-Vaida, Z. Wang, V. S. B. Shankar, L. Ruwe, C. A. Taatjes, P. Dagaut, N. Hansen. *J. Phys. Chem. A* **120**, 7890 (2016).
[98] L.-S. Tran, J. Pieper, H.-H. Carstensen, H. Zhao, I. Graf, Y. Ju, F. Qi, K. Kohse-Höinghaus. *Proc. Combust. Inst.* **36**, 1165 (2017).
[99] Y. Sakai, J. Herzler, M. Werler, C. Schulz, M. Fikri. *Proc. Combust. Inst.* **36**, 195 (2017).

[100] L.-S. Tran, O. Herbinet, Y. Li, J. Wullenkord, M. Zeng, E. Bräuer, F. Qi, K. Kohse-Höinghaus, F. Battin-Leclerc. *Proc. Combust. Inst.* (2018). https://doi.org/10.1016/j.proci.2018.05.135.
[101] S. Thion, C. Togbé, Z. Serinyel, G. Dayma, P. Dagaut. *Combust. Flame* **185**, 4 (2017).
[102] L. Cai, A. Sudholt, D. J. Lee, F. N. Egolfopoulos, H. Pitsch, C. K. Westbrook, S. M. Sarathy. *Combust. Flame* **161**, 798 (2014).
[103] J. Wullenkord, L.-S. Tran, J. Böttchers, I. Graf, K. Kohse-Höinghaus. *Combust. Flame* **190**, 36 (2018).
[104] L. Lautenschütz, D. Oestreich, P. Seidenspinner, U. Arnold, E. Dinjus, J. Sauer. *Fuel* **173**, 129 (2016).
[105] M. Härtl, P. Seidenspinner, E. Jacob, G. Wachtmeister. *Fuel* **153**, 328 (2015).
[106] N. Mahbub, A. O. Oyedun, A. Kumar, D. Oestreich, U. Arnold, J. Sauer. *J. Cleaner Prod.* **165**, 1249 (2017).
[107] A. Omari, B. Heuser, S. Pischinger. *Fuel* **209**, 232 (2017).
[108] W. Sun, T. Tao, M. Lailliau, N. Hansen, B. Yang, P. Dagaut. *Combust. Flame* **193**, 491 (2018).
[109] F. H. Vermeire, H.-H. Carstensen, O. Herbinet, F. Battin-Leclerc, G. B. Marin, K. M. Van Geem. *Combust. Flame* **190**, 270 (2018).
[110] W. A. Kopp, L. C. Kröger, M. Döntgen, S. Jacobs, U. Burke, H. J. Curran, K. A. Heufer, K. Leonhard. *Combust. Flame* **189**, 433 (2018).
[111] W. Sun, G. Wang, S. Li, R. Zhang, B. Yang, J. Yang, Y. Li, C. K. Westbrook, C. K. Law. *Proc. Combust. Inst.* **36**, 1269 (2017).
[112] U. Burke, K. P. Somers, P. O'Toole, C. M. Zinner, N. Marquet, G. Bourque, E. L. Petersen, W. K. Metcalfe, Z. Serinyel, H. J. Curran. *Combust. Flame* **162**, 315 (2015).
[113] P. Dagaut, C. Togbé. *Fuel* **89**, 280 (2010).
[114] M. Salamanca, J. Wullenkord, I. Graf, S. Schmitt, L. Ruwe, K. Kohse-Höinghaus. *Proc. Combust. Inst.* (2018). https://doi.org/10.1016/j.proci.2018.05.111.
[115] K. O. Johansson, F. El Gabaly, P. E. Schrader, M. F. Campbell, H. A. Michelsen. *Aerosol Sci. Technol.* **51**, 1333 (2017).
[116] Y. Wang, S. Park, S. M. Sarathy, S. H. Chung. *Combust. Flame* **192**, 71 (2018).
[117] D. Aubagnac-Karkar, A. El Bakali, P. Desgroux. *Combust. Flame* **189**, 190 (2018).
[118] M. R. Kholghy, G. A. Kelesidis, S. E. Pratsinis. *Phys. Chem. Chem. Phys.* **20**, 10926 (2018).
[119] T. Zhang, M. J. Thomson. *Combust. Flame* **190**, 416 (2018).
[120] C. Saggese, S. Ferrario, J. Camacho, A. Cuoci, A. Frassoldati, E. Ranzi, H. Wang, T. Faravelli. *Combust. Flame* **162**, 3356 (2015).
[121] P. Desgroux, A. Faccinetto, X. Mercier, T. Mouton, D. Aubagnac Karkar, A. El Bakali. *Combust. Flame* **184**, 153 (2017).
[122] N. D. Loh, C. Y. Hampton, A. V. Martin, D. Starodub, R. G. Sierra, A. Barty, A. Aquila, J. Schulz, L. Lomb, J. Steinbrener, R. L. Shoeman, S. Kassemeyer, C. Bostedt, J. Bozek, S. W. Epp, B. Erk, R. Hartmann, D. Rolles, A. Rudenko, B. Rudek, L. Foucar, N. Kimmel, G. Weidenspointner, G. Hauser, P. Holl, E. Pedersoli, M. Liang, M. M. Hunter, L. Gumprecht, N. Coppola, C. Wunderer, H. Graafsma, F. R. N. C. Maia, T. Ekeberg, M. Hantke, H. Fleckenstein, H. Hirsemann, K. Nass, T. A. White, H. J. Tobias, G. R. Farquar, W. H. Benner, S. P. Hau-Riege, C. Reich, A. Hartmann, H. Soltau, S. Marchesini, S. Bajt, M. Barthelmess, P. Bucksbaum, K. O. Hodgson, L. Strüder, J. Ullrich, M. Frank, I. Schlichting, H. N. Chapman, M. J. Bogan. *Nature* **486**, 513 (2012).
[123] A. Liati, D. Schreiber, Y. Arroyo Rojas Dasilva, P. Dimopoulos Eggenschwiler. *Environ. Pollut.* **239**, 661 (2018).
[124] B. Giechaskiel, J. Vanhanen, M. Väkevä, G. Martini. *Aerosol Sci. Technol.* **51**, 626 (2017).
[125] A. Liati, D. Schreiber, P. Dimopoulos Eggenschwiler, Y. Arroyo Rojas Dasilva, A. C. Spiteri. *Combust. Flame* **166**, 307 (2016).
[126] G. Kalghatgi. *Appl. Energy* **225**, 965 (2018).
[127] C. Zamfirescu, I. Dincer. *Fuel Process. Technol.* **90**, 729 (2009).
[128] R. Lan, J. T. S. Irvine, S. Tao. *Int. J. Hydrogen Energy* **37**, 1482 (2012).
[129] W. I. F. David, J. W. Makepeace, S. K. Callear, H. M. A. Hunter, J. D. Taylor, T. J. Wood, M. O. Jones. *J. Am. Chem. Soc.* **136**, 13082 (2014).
[130] A. Afif, N. Radenahmad, Q. Cheok, S. Shams, J. H. Kim, A. K. Azad. *Renew. Sustain. Energy Rev.* **60**, 822 (2016).
[131] E. C. Okafor, Y. Naito, S. Colson, A. Ichikawa, T. Kudo, A. Hayakawa, H. Kobayashi. *Combust. Flame* **187**, 185 (2018).
[132] K. D. K. A. Somarathne, S. Hatakeyama, A. Hayakawa, H. Kobayashi. *Int. J. Hydrogen Energy* **42**, 27388 (2017).
[133] A. Valera-Medina, R. Marsh, J. Runyon, D. Pugh, P. Beasley, T. Hughes, P. Bowen. *Appl. Energy* **185**, 1362 (2017).
[134] A. Ichikawa, A. Hayakawa, Y. Kitagawa, K. D. K. A. Somarathne, T. Kudo, H. Kobayashi. *Int. J. Hydrogen Energy* **40**, 9570 (2015).
[135] Y. Liu, X. Sun, V. Sethi, D. Nalianda, Y.-G. Li, L. Wang. *Prog. Aerospace Sci.* **94**, 12 (2017).
[136] H. Lund, P. A. Østergaard, D. Connolly, B. V. Mathiesen. *Energy* **137**, 556 (2017).
[137] L. Tartakovsky, M. Sheintuch. *Prog. Energy Combust. Sci.* **67**, 88 (2018).
[138] J. Herzler, Y. Sakai, M. Fikri, C. Schulz. *Proc. Combust. Inst.* (2018). https://doi.org/10.1016/j.proci.2018.05.120.
[139] F. Sen, B. Shu, T. Kasper, J. Herzler, O. Welz, M. Fikri, B. Atakan, C. Schulz. *Combust. Flame* **169**, 307 (2016).
[140] D. Nativel, B. Shu, J. Herzler, M. Fikri, C. Schulz. *Proc. Combust. Inst.* (2018). https://doi.org/10.1016/j.proci.2018.06.083.
[141] S. Wiesmann, R. Hegner, B. Atakan, C. Schulz, S. Kaiser. *Fuel* **215**, 40 (2018).
[142] H. Brunner, M. Hirz, W. Hirschberg, K. Fallast. *Energy Sust. Soc.* **8:9** (2018). https//doi.org/10.1186/s13705-018-0149-0.
[143] J. G. Anderson, C. E. Clapp. *Phys. Chem. Chem. Phys.* **20**, 10569 (2018).
[144] http://www.elysee.fr/declarations/article/transcription-du-discours-du-president-de-la-republique-emmanuel-macron-devant-le-congres-des-etats-unis-d-amerique/April 25, 2018 (accessed June 20, 2018).